NeuroImage 274 (2023) 120150

Contents lists available at ScienceDirect

NeuroImage

journal homepage: www.elsevier.com/locate/neuroimage

Adaptive coding of stimulus information in human frontoparietal cortex during visual classification

David Wisniewski[a,b,*], Carlos González-García[a,c,d], Silvia Formica[a,b], Alexandra Woolgar[e], Marcel Brass[a,b]

[a] Department of Experimental Psychology, Ghent University, Ghent, Belgium
[b] Berlin School of Mind and Brain/ Department of Psychology, Humboldt University of Berlin, Federal Republic of Germany
[c] Mind, Brain and Behavior Research Center, University of Granada, Spain
[d] Department of Experimental Psychology, University of Granada, Spain
[e] Medical Research Council Cognition and Brain Sciences Unit, University of Cambridge, UK

ARTICLE INFO

Keywords:
fMRI
RSA
Frontoparietal cortex
Multiple demand
Perceptual classification

ABSTRACT

The neural mechanisms of how frontal and parietal brain regions support flexible adaptation of behavior remain poorly understood. Here, we used functional magnetic resonance imaging (fMRI) and representational similarity analysis (RSA) to investigate frontoparietal representations of stimulus information during visual classification under varying task demands. Based on prior research, we predicted that increasing perceptual task difficulty should lead to adaptive changes in stimulus coding: task-relevant category information should be stronger, while task-irrelevant exemplar-level stimulus information should become weaker, reflecting a focus on the behaviorally relevant category information. Counter to our expectations, however, we found no evidence for adaptive changes in category coding. We did find weakened coding at the exemplar-level within categories however, demonstrating that task-irrelevant information is de-emphasized in frontoparietal cortex. These findings reveal adaptive coding of stimulus information at the exemplar-level, highlighting how frontoparietal regions might support behavior even under challenging conditions.

1. Introduction

Regardless of the context we might find ourselves in, we can often adjust our behavior to current demands (Fuster, 2000; Miller, 2000), an ability that is supported by a set of frontal and parietal brain regions often called the multiple demand (MD) network (Duncan, 2010; Fedorenko et al., 2013). Past research using multivariate decoding (Haynes, 2015; Kamitani and Tong, 2006) revealed that MD regions encode a wide range of task-related information, including stimuli (Ashby and Zeithamova, 2022), responses, and task-rules (Woolgar et al., 2016). Such representations can be described in terms of their coding strength (operationalized *via* e.g. decoding accuracies) and their coding format (i.e. their representational geometry, Kriegeskorte and Kievit 2013). Coding in MD regions is stronger for behaviorally relevant information that is explicitly attended (Jackson et al., 2017; Jackson and Woolgar, 2018; Woolgar et al., 2015b), when performance is rewarded (Etzel et al., 2016), or whenever tasks are particularly difficult (Jackson et al., 2021; Woolgar et al., 2011a, 2015a). This has been taken as evidence for adaptive coding (Duncan, 2010), i.e. the existence of multi-modal neurons rapidly and flexibly changing their coding properties to meet current demands. In turn these neurons are thought to bias coding in sensory and motor regions (Desimone and Duncan, 1995; Duncan, 2013). However, other research demonstrated that, at least under some conditions, coding strength and formats of task-related information in MD cortex does not adapt to changing demands (Loose et al., 2017; Wisniewski et al., 2016, 2019), and instead the same representations are re-used regardless of the current context. Perceptual difficulty is a particularly interesting case here, since some researchers have suggested that MD cortex is unable to adapt to changes in the quality of perceptual input (Wen et al., 2018), while others have demonstrated adaptive coding under varying perceptual difficulties (Woolgar et al., 2011a, 2015a). Thus, it remains an open question whether adaptive coding is a general property of these regions, or whether frontoparietal cortex only adapts its representations under specific circumstances, and instead re-uses the same representations when necessary (Badre et al., 2021; Botvinick and Cohen, 2014; Wisniewski, 2018).

Previous research focused primarily on investigating *whether* coding adapts to different demands, for instance by testing whether information coding is stronger on hard than on easy trials (Woolgar et al., 2011a), or

* Corresponding author at: Department of Experimental Psychology, Ghent University, Henri Dunantlaan 2, Ghent, Belgium.
E-mail address: david.wisniewski@ugent.be (D. Wisniewski).

https://doi.org/10.1016/j.neuroimage.2023.120150.
Received 20 October 2022; Received in revised form 19 April 2023; Accepted 29 April 2023
Available online 30 April 2023.

stronger in freely chosen than in externally cued tasks (Wisniewski et al., 2016; Zhang et al., 2013). These studies have been optimized to detect the presence or absence of differences in coding strength across conditions, often using multivariate decoding methods (Kamitani and Tong, 2006), but make no explicit predictions about the representational formats used in each condition. Yet, changes to coding strength do not necessarily imply changes in coding format as well, and it remains difficult to draw strong conclusions about *how* representational formats change across conditions (e.g. more or less categorical coding). A complete explanation of how adaptive changes in neural coding are related to behavior requires both a description of changes to coding strength *and* format. We argue that understanding adaptive coding at the level of representational formats remains key to understanding the neural basis of goal-directed behavior.

Here, we used a visual classification task (Li et al., 2007) and assessed coding formats, to directly tackle this issue. In the past, visual classification was used successfully to study the representational format of task-related stimulus information in non-human primates (Brincat et al., 2018; Freedman et al., 2003), dissociating exemplar-level and category-level stimulus coding. One of the key findings was that sensory and frontoparietal brain regions emphasize different aspects of the stimulus information (Freedman et al., 2003). Sensory regions preserved exemplar-level stimulus information, even if this was not task-relevant since classification is possible without differentiating individual exemplars within the same category (Eger et al., 2008). Frontoparietal brain regions more strongly represented task-relevant category information (Heekeren et al., 2004), with much less exemplar-level information. This is usually interpreted as evidence for more abstract, behaviorally optimized stimulus coding in frontoparietal cortex (Brincat et al., 2018). Here, we tested whether these results also obtained in population-level information coding in humans, and asked how these coding properties change when the perceptual difficulty of the task changed. Given the previous findings, we had three main hypotheses.

First, we expected that visual regions would encode category-level stimulus information on perceptually easy trials. Increasing perceptual difficulty by adding noise to the stimuli was expected to weaken category coding in visual regions (Hypothesis 1). Second, we expected to find category coding in MD regions (Jackson et al., 2017, 2021; Jackson and Woolgar, 2018, Woolgar et al., 2011b), but also expected a different effect of perceptual difficulty. Since coding of task-related information in MD regions is stronger on difficult trials (Woolgar et al., 2011a, 2015a), category coding should be relatively weak on perceptually easy trials (Hypothesis 2), and stronger on perceptually difficult trials here as well. Third, we expected representational formats to become more clustered, i.e. the differences between individual exemplars within a category should grow smaller with increasing difficulty (Hypothesis 3). De-emphasizing the task-irrelevant exemplar-level information can be seen as a means to optimize stimulus representations to support behavior in this classification task. Note that previously reported increase in decoding accuracy might be driven by both, stronger category separation and/or more clustered exemplar representations. Using RSA, we can assess both, helping us to better understand the neural mechanisms of how MD regions support adaptive behavior, especially under difficult conditions.

2. Methods

2.1. Participants

Forty-nine volunteers (38 female, 11 male, mean age: 24.1 years, range: 18–36 years) with normal or corrected-to-normal vision participated in the study. We obtained written informed consent from each participant prior to participation, and the Ethics Committee of the Ghent University Hospital approved this experiment (project identifier BC-07446). Each volunteer received 43€ for their participation. We first calculated the average error rate for each participant in the easiest possible condition in this experiment (clean template images, see below for more details). Five participants had excessive error rates (above 1.5*IQR of the group mean,): 10.4%, 10.4%, 12.5%, 16.7%, and 22.9% respectively, group average = 3.1%. These participants were excluded from the sample. Four participants showed excessive head movement during scanning (> 5 mm), and were also removed. Two additional subjects were removed due to technical difficulties. The final sample consisted of thirty-eight participants (29 female, 9 male, mean age = 24.4 years, range: 19–36 years).

2.2. Task: stimuli and design

Stimuli consisted of gradually morphed, greyscale images, created using 3 cat templates to 3 dog templates (Fig. 1A), two of which were randomly chosen for each participant. Stimuli were created by linearly combining one cat and one dog template, with changing contributions (morph level, e.g. 93.4% cat, 6.6% dog, with steps of 6.6). These stimuli have been used before in non-human primate research, and for more detail on their generation see (McKee et al., 2014). For each combination of cat and dog templates, 16 stimuli were created (8 dog + 8 cat stimuli). Each stimulus was categorized as either cat or dog depending on which category contributed more to the image (>50%). This yielded 32 cat and 32 dog stimuli, which differed in their distance to the category boundary (choice difficulty). We then added random Gaussian noise to these images, making classification more difficult (noise level). The amount of added noise was adapted to each participant using a staircase procedure (see below). This resulted in a 2 (categories) x 8 (choice difficulties) x 2 (noise levels) x 4 (template combinations) design with 128 unique stimuli. In order to increase the signal-to-noise ratio and have more trials in each cell of the design matrix, we then collapsed across all template combinations, and collapsed data from eight to four choice difficulty levels for all analyses.

2.3. Procedure

The experiment was programmed using PsychoPy3 (v.2020.1.3, Peirce 2007). Participants started by performing a short training session outside the MR scanner, where they received trial-by-trial feedback on their responses. They first learned to classify template images, followed by classifying clean morphed images. They then entered the MR scanner, where they completed a staircase procedure to calibrate the noise level in the scanning environment. For this purpose, we presented template stimuli with varying levels of random Gaussian noise added. After each correct response, noise increased. After each wrong response, noise decreased. After seven reversals of noise change direction (up → down, down → up), the staircase procedure stopped and we applied the final noise level to all noisy stimuli used in the experiment.

After that, participants performed 6 runs of 128 trials of the experimental task. In each trial, a stimulus was presented on screen for 1.8 s (Fig. 1B), which was followed by a variable, pseudo-exponentially distributed inter-trial-interval (ITI, mean duration = 2.7 s, range between 0.8 s and 10.4 s). Participants were instructed to respond while the stimulus was presented on screen, as quickly and accurately as possible. As an additional incentive, participants that were among the top 20% fastest *and* top 20% most accurate received a 10€ bonus payment. Participants responded using the left and right index fingers, using MR-compatible response boxes. Category-button-mappings were counterbalanced across runs for each participant (dog: right, cat: left in half of the runs, dog: left, cat: right in the other half). Participants received feedback at the end of each run (mean error rate + mean reaction time).

In each run, each unique stimulus was presented once, resulting in 8 repetitions of each combination of category (2), choice difficulty (4), and noise level (2). Category, choice difficulty, and template combination were pseudo-randomized and changed on a trial-by-trial basis. Noise level was blocked, and each run consisted of 4 blocks of 32 trials each. Two blocks were noisy, two blocks were clean, and half of the

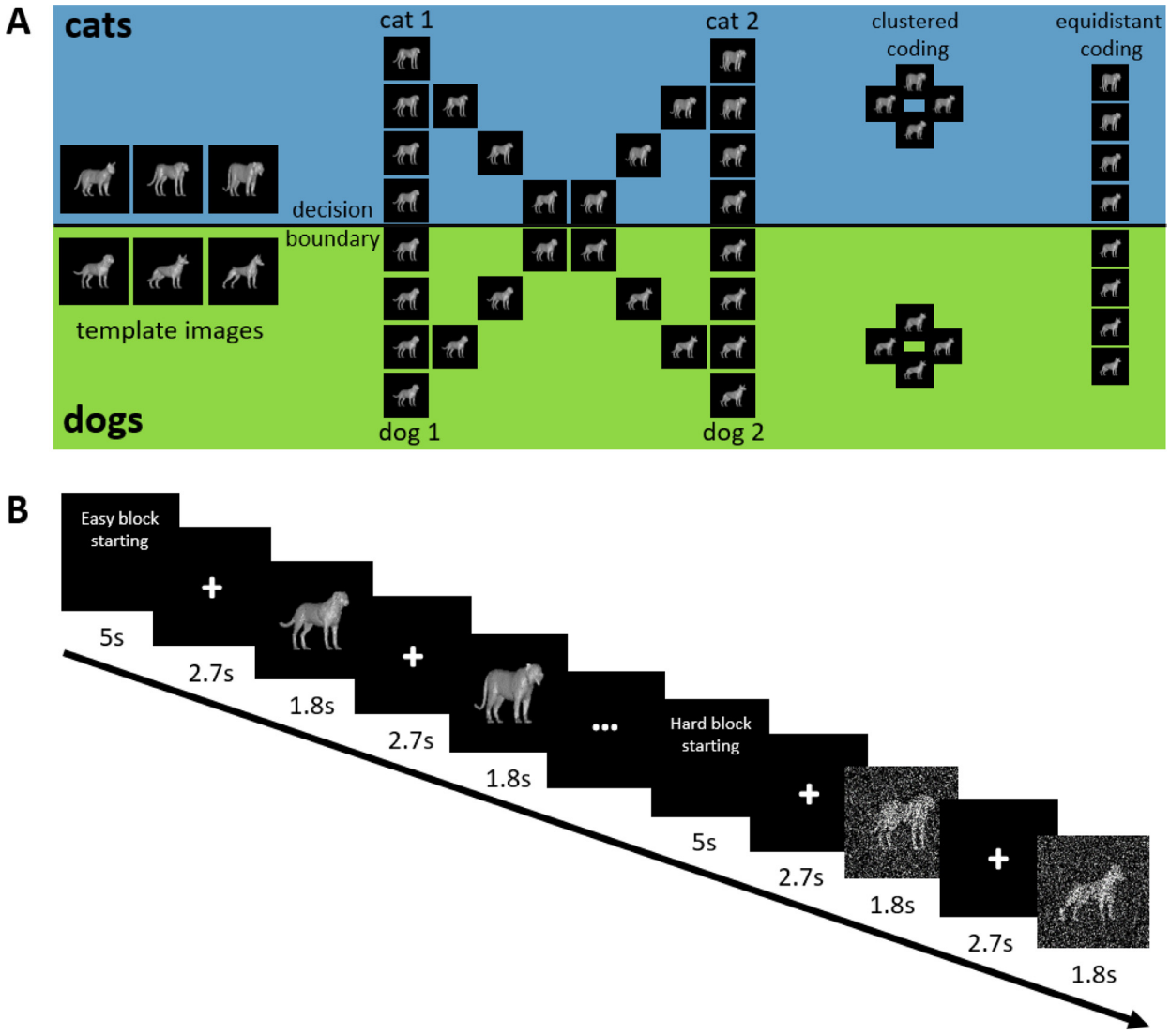

Fig. 1. *Experimental design.* A. *Stimuli.* On the left, all template images used here are depicted. All stimuli above the decision boundary are cats, all below are dogs. Each participant was presented 2 out of 3 cat/dog templates (randomly selected for each participant). In the middle, example morphed stimuli are depicted for 2 dog and 2 cat template images. On the right, a schematic representation of clustered and equidistant coding is depicted. When stimulus representations are clustered, representational distances between exemplars of the same category (e.g. dog) are small, i.e. representations are highly similar. Distances between categories are large. When stimulus representations are equidistant, distances from the perceptual space (middle) are preserved in the neural space, including differences between exemplars within the same category. B. *Trial timing.* Each block started with an instruction screen. Then, stimuli were presented for 1.8 s, interleaved with a variable inter-trial-interval (mean duration 2.7 s, range 0.8 – 10.4 s).

runs started with a noisy block, while the other half started with a clean block. Each block started with an instruction screen presented for 5 s ('Easy block starting', 'Hard block starting'). We then ensured that none of the design variables was correlated, and that there were no sequential dependencies between trials, using a mutual information criterion (using permutation tests, $p > 0.005$).

Due to a coding error, for the first 29 participants, designs contained different numbers of cat and dog stimuli in each run, for each combination of choice difficulty and noise level. This introduced additional noise to the data, and made signal estimation in some conditions and some runs more difficult. However, due to the mutual information testing we employed before accepting designs, we ensured that this did not introduce any systematic biases even within participants.

2.4. Image acquisition

Functional imaging was performed on a 3T Siemens Prisma MRI scanner (Siemens Medical Systems, Erlangen, Germany), using a 64-channel head coil. For each of the six functional scanning runs, we acquired 350 T2*-weighted whole-brain echo-planar images (EPI, TR = 1730 ms, TE = 30 ms, image matrix = 84 × 84, FOV = 210 mm, flip angle=66°, slice thickness = 2.5 mm, voxel size = 2.5 × 2.5 × 2.5 mm, distance factor=0%, 50 slices with slice acceleration factor 2). Slices were oriented along the AC-PC line for each participant. A T1-weighted structural scan was acquired prior to the functional scans (MPRAGE, TR = 2250 ms, TE = 4.18 ms, TI = 900 ms, acquisition matrix = 256 × 256, FOV = 256 mm, flip angle=9°, voxel size = 1 × 1 × 1 mm). We further acquired 2 field maps (phase and magnitude) to correct for inhomogeneities in the magnetic field (TR = 520 ms, TE1 = 4.92 ms, TE2 = 7.38 ms, image matrix = 70 × 70, FOV = 210 mm, flip angle=60°, slice thickness = 3 mm, voxel size = 3 × 3 × 2.5 mm, distance factor=0%, 50 slices).

2.5. Analysis: behavior

Behavioral data were analyzed using RStudio (version 1.2.1335, R version 4.0.3). We first removed all trials on which the participant failed to respond. On average, we removed 1.66% (SD = 0.64%) of all trials

for each participant this way. Additionally, we removed trials with RTs < 150 ms, removing 1.68% of trials on average (SD = 0.64%). To assess task performance, we extracted mean RTs and error rates for each combination of noise level and choice difficulty. For the RT analysis, we only used correct responses. RTs were then entered into a Bayesian ANOVA (*BayesFactor::anovaBF*, using the default scaled inverse chi-square prior on main effects and interactions, scaling factor fixed effects = 0.5, scaling factor random effects = 1), testing for evidence for or against both main effects and their interaction. Participants were entered as a random effect into this model. We interpreted the resulting Bayes Factors (BF10) according to Wagenmakers (2007). The same procedure was then applied to error rates.

We additionally fitted psychometric functions to the choice data, separately for each participant (Weibull function, using *quickpsy*, Linares and López-Moliner 2016). Specifically, we computed the probability of choosing the dog response separately for each combination of morph level and noise level, and then fitted psychometric functions separately for both noise levels. This allowed us to extract several key parameters from the choice data: k, guess rate, and threshold. k determines the slope of the psychometric function and describes how sharply both categories are distinguished. The guess rate quantifies how often participants guess, and we expected k to be lower and the guess rate to be higher on noisy, as compared to clean, trials. To test this hypothesis, we entered estimates into a Bayesian paired t-test (*BayesFactor::ttestBF*, Cauchy prior, scaling factor = 0.707), comparing parameter values across noise levels. The threshold quantifies at which point on the scale of morphed images, ranging from 100% cat to 100% dog, participants were equally likely to choose cat or dog. We expected this to fall in the middle of the scale, i.e. where stimuli are close to 50% cat / 50% dog, and tested this hypothesis using a Bayesian t-test (Cauchy prior, scaling factor = 0.707).

2.6. Analysis: fMRI

fMRI analyses were performed using Matlab (R2018b, version 9.5.0.944444, The Mathworks), SPM12 (https://www.fil.ion.ucl.ac.uk/spm/), The Decoding Toolbox (v 3.99, Hebart et al. 2014), and RStudio (version 1.2.1335, R version 4.0.3). Raw data were first unwarped, realigned, and slice-time corrected (code: https://github.com/CCN-github/fMRI-preprocessing-SPM12). We then estimated normalization fields for each participant, which were used to project mask files from normalized to native space. No spatial smoothing or normalization was applied to BOLD data to preserve fine-grained voxel activation patterns.

2.6.1. First-level GLM analysis

Preprocessed data were used to estimate a voxel-wise general linear model (GLM, Friston et al. 1994). Sixteen regressors of interest were used, one for each combination of category (cat, dog), noise level (clean, noisy), and choice difficulty (1, 2, 3, 4). We then added a variable number of nuisance regressors for each participant. First, we added condition-specific error regressors, modelling error trials separately for each condition. This led to a variable number of nuisance regressors, since not every run had errors in each condition. We chose condition-specific error regressors over a single error regressor, since we expected errors in very easy trials to derive from different psychological processes than in very difficult trials (e.g. momentary lapse in attentional processes vs guessing). Second, we added six movement regressors. Regressors were time-locked to the onset of the stimulus presentation. We used the finite impulse response function as a basis function (FIR, 5 time bins with a duration of 1.73 s each). This makes fewer assumptions about the shape of the haemodynamic response, compared to a canonical haemodynamic response function, making it better suited to model responses to short events in a heterogeneous set of brain regions from visual to prefrontal cortex (see Wisniewski et al. 2015 for a similar approach).

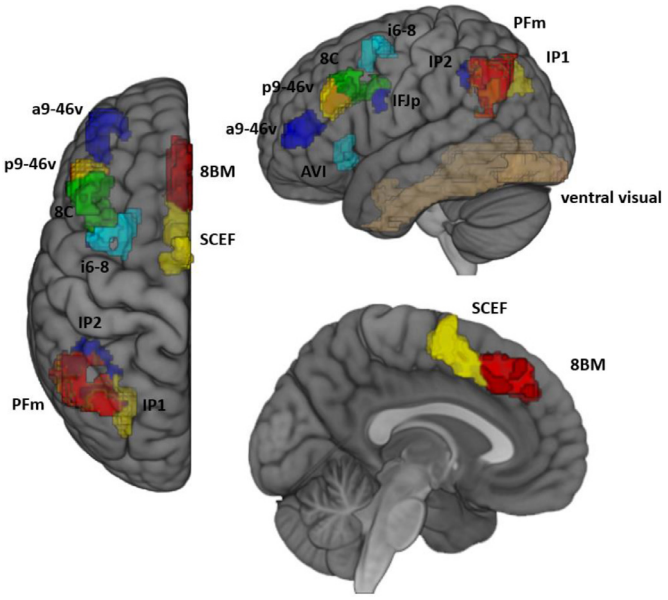

Fig. 2. *ROIs.* ROIs were derived from the HCP atlas (Glasser et al., 2016) and included the multiple demand regions identified in Assem et al. (2020). The ventral visual cortex ROI was defined using the Harvard-Oxford atlas.

2.5.2. Feature selection

ROI selection: Similar to Assem et al. (2020), we defined a number of a-priori volumetric multiple demand (MD) regions-of-interest (ROIs), based on the Human Connectome Project atlas. The following regions were included in this experiment: SCEF, 8BM, 8C, IFJp, p9_46v, a9_46v, i68, AVI, IP1, IP2, PFm (see Fig. 2, code: https://github.com/davidwisniewski/fmri-extract-HCP-mask). As an additional region of interest, we used the ventral visual cortex, as defined using the Harvard-Oxford atlas. Data from the chosen ROIs was extracted in native space for each subject, by projecting the ROI masks from MNI to native space separately for each participant, using the inverse normalization fields estimated during pre-processing.

Time-bin selection: Given that we use the FIR basis function, each regressor is modelled at five different time points. To select a time window of interest, we first estimated the haemodynamic lag to be 2TRs (3.46 s), based on previous research using MVPA methods to extract task-related information from frontoparietal cortex (Bode and Haynes, 2009; Momennejad and Haynes, 2013; Wisniewski et al., 2015). We then corrected for haemodynamic lag by using data from time bins 3 and 4, which started 3.46 s and 5.19 s after stimulus onset, respectively, for all multivariate pattern analyses. Again, this follows past research on time-resolved pattern analysis of task-related information (Momennejad and Haynes, 2012). We expected haemodynamic responses to be short, given that the trial duration / stimulus processing was short, and this procedure strikes a balance between accounting for the expected short duration, and still allowing for the peak response to occur within a variable time window (between 3.46 s and 6.92 s after stimulus onset).

2.5.3. Representational similarity analysis

For each ROI, we first extracted the beta weights for the 16 regressors of interest in each run. We then used The Decoding Toolbox (Hebart et al., 2014) to perform a representational similarity analysis (RSA, Kriegeskorte et al. 2008, Nili et al. 2014), using run-wise cross-validated Euclidean distance measures and applying multivariate noise normalization (Walther et al., 2016). Using cross-validated distances ensures that estimates are unbiased and average to zero if there is no systematic relation between activation patterns (Arbuckle et al., 2019). All computed distances were then converted to a 16 × 16 representational

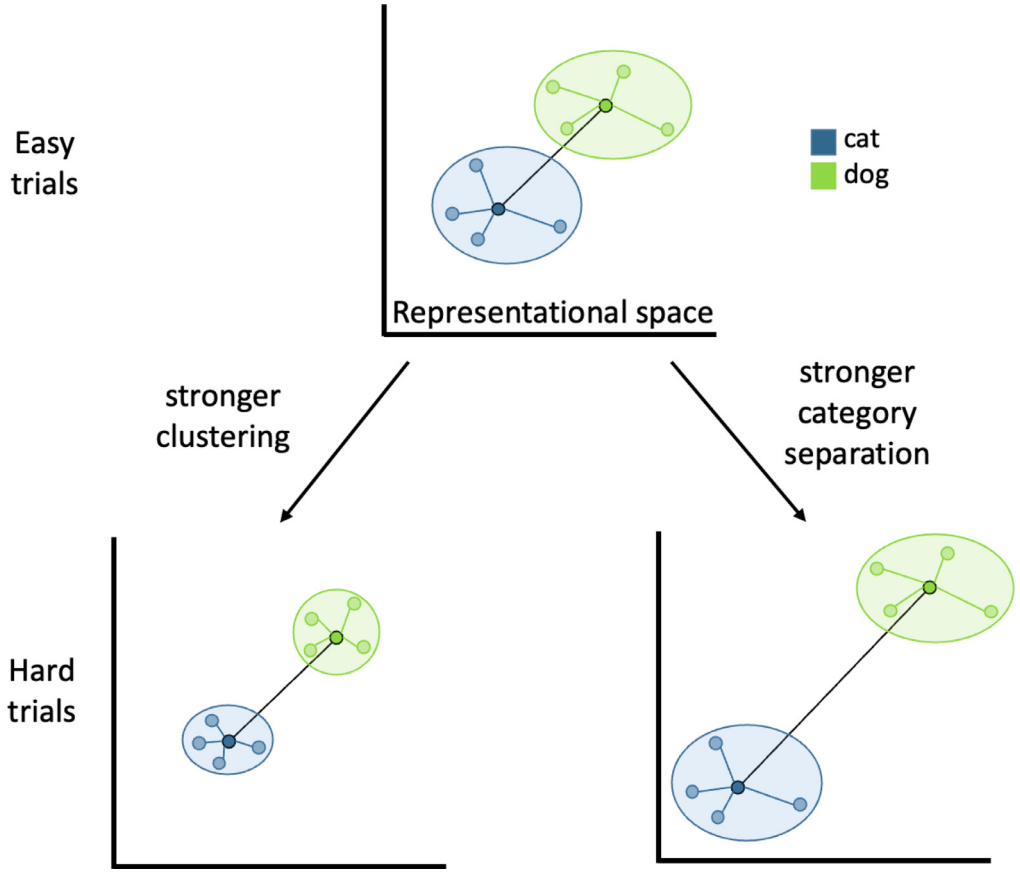

Fig. 3. *Schematic of our analysis approach*. For each ROI, we computed a 16 × 16 representational distance matrix, using cross-validated Euclidean distances. From this matrix, we computed the centroids of the stimuli in each category separately, finding the center of all e.g. dog stimuli in the neural state space. The distance between both centroids was used to measure category separation. Then, we computed the distances of each exemplar to their respective centroid, which served as a measure of clustering within categories. We expected increased perceptual difficulty to lead to stronger category separation (lower right), and to stronger clustering (lower left) in MD regions.

distance matrix (RDM), representing pairwise distances between all conditions. This procedure was performed separately for each ROI, and for each of the two time bins of interest. For each ROI, we then averaged the RDMs across both time bins.

The main goal of this experiment was to identify whether and how stimulus information was encoded in the MD network at the category and exemplar level. For this purpose, we leveraged the fact that each RDM constitutes a high-dimensional Euclidean space, allowing us to measure distances between exemplars within that space (using *usedist*). Based in these distance measures, we computed measures to separately assess stimulus coding at the category and exemplar level in each ROI and in both perceptual difficulty conditions (Fig. 3).

In order to determine the strength of the category-level signal, we first computed the centroid of all cat stimuli, and the centroid of all dog stimuli. This is similar to computing centroids in e.g. k-means clustering algorithms, and measures the center of the distribution of all cat/dog stimuli in representational space. After computing the cat and dog centroids, we computed the Euclidean distance between these two points, yielding a direct measure of the representational distance between cats and dogs in this experiment. If this measure was larger than zero (across all participants), this would indicate the presence of category-level stimulus coding. This "centroid distance" analysis was performed separately for clean and noisy trials.

In order to determine the strength of the exemplar-level signal, we again computed the centroid location for both categories, and then computed the distance of each exemplar to its respective centroid (i.e. cat1 to cat centroid, dog1 to dog centroid, etc). These exemplar-to-centroid distances were then averaged to generate an index of how much individual exemplars spread around the category centroids. High values indicated less clustering and higher distances between individual exemplar, low values indicated more clustering and lower distances between individual exemplars. Again, this analysis was performed separately for clean and noisy trials. We refer to this measure as "clustering index".

2.5.5. Hypothesis 1: visual cortex encodes category-level stimulus information

To test this hypothesis, we first tested whether the centroid distance in ventral visual cortex was larger than zero, using a Bayesian one-sided t-test (*BayesFactor::ttestBF*, Cauchy prior, scaling factor = 0.707). Then, we tested whether the clustering index was larger than zero, again using a Bayesian one-sided t-test. We expected to find evidence for the alternative hypothesis in both tests. Furthermore, we expected to see weaker category-level stimulus coding on noisy, as compared to clean trials. This was tested by comparing the centroid distance across perceptual difficulty levels using a one-sided paired Bayesian t-test.

2.5.6. Hypothesis 2: stronger category signals on noisy trials in MD regions

On both clean and noisy trials, we expected MD regions to encode category-level stimulus information. To test this hypothesis, we assessed whether centroid distances were larger than zero in each ROI and each perceptual difficulty condition, using one-sided Bayesian t-tests. We further expected category signals to be stronger on noisy than on clean trials. This was tested using one-sided paired Bayesian t-tests.

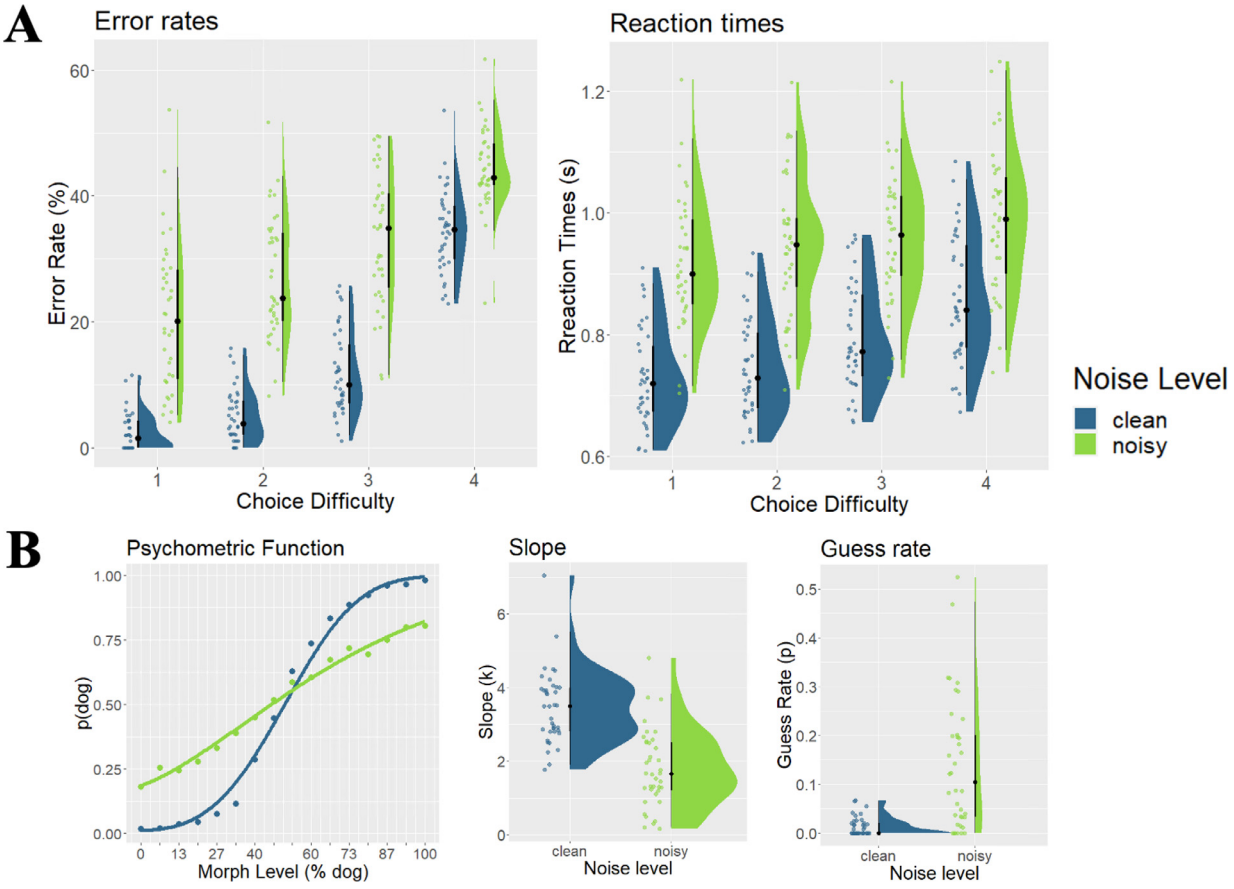

Fig. 4. *Behavioral Results*. A. *Error rates and reaction times*. Plots show error rates (left) and reaction times (right) as a function of choice difficulty (1 = easy / far away from decision boundary, 4 = hard / close to decision boundary). Raincloud plots include boxplots centered around the median (black lines), probability density estimates (right half), and raw data (left half), jittered for illustration purposes. B. *Psychometric functions*. Group-average choice data is shown on the left. Each dot represents the probability of choosing 'dog' (p(dog)), as a function of morph level (expressed in% dog included in the morphed image). Lines represent fitted psychometric functions. Estimated slope (k) and guess rate parameters from the psychometric curve are shown on the right, as a function of noise level (clean, noisy). blue = clean trials, green= noisy trials.

2.5.7. Hypothesis 3: more clustering on noisy trials in MD regions

Lastly, we hypothesized that the representational format would shift towards more clustered stimulus representations on noisy trials. To test this hypothesis, we performed a one-sided paired Bayesian t-test, comparing the clustering index across clean and noisy trials. Taking Hypotheses 2 and 3 together, we essentially hypothesized that MD regions would adapt to increased difficulty by emphasizing task-relevant category information (Hypothesis 2) while simultaneously de-emphasizing task-irrelevant exemplar information (Hypothesis 3).

3. Results

3.1. Behavioral results

We first characterized behavioral performance by collapsing data across both categories, and then computing a 2 (noise level) x 4 (choice difficulty) Bayesian ANOVA on the error rates (Fig. 4A, left panel). We found performance to range from 2.33% errors to 44.25% errors, and found very strong evidence for main effects of both noise level and choice difficulty, BF10s > 150, with noisy trials and high choice difficulty trials having higher error rates. The effect of noise level decreased with increasing choice difficulty (interaction effect, BF10 > 150), likely reflecting a floor effect in performance, with classification on stimuli very close to the decision boundary being so difficult that adding noise had a negligible effect on performance. We found similar results for reaction times (Fig. 4A, right panel), with very strong evidence for both main effects, BF10 > 150, and strong evidence for an interaction effect, BF10 = 80.51. Only correct trials were used in RT analyses.

Next, we assessed performance by fitting psychometric functions to the choice data of each participant (Fig. 4B). We first tested whether the slope of the function was higher on clean than on noisy trials, which would indicate a sharper category separation. We found very strong evidence for this effect, BF10 > 150 (mean $slope_{clean}$ = 3.48, mean $slope_{noisy}$ = 1.81). We then tested whether choices were biased towards either cats or dogs by analyzing the threshold parameter of the psychometric function, and found no evidence for biased choices in either clean or noisy trials (Supplementary Analysis 1). Lastly, we investigated whether the guess rate (proportion of trials in which participants guessed) was higher on noisy than on clean trials. We found very strong evidence for this effect, BF10 > 150 (mean $guess_{clean}$ = 0.01, mean $guess_{noisy}$ = 0.13), showing that overall, adding noise led to substantially more guessing, and a weaker separation of both categories.

3.2. Hypothesis 1: visual cortex encodes category-level stimulus information

We first tested whether the visual cortex encoded category-level stimulus information, separately for clean and noisy trials. We found strong evidence for an effect on both clean and noisy trials, BF10s > 150 (Fig. 5). We then hypothesized that category information would be weaker on noisy than on clean trials in visual cortex, since stimuli were severely degraded. Unexpectedly, we found evidence against a

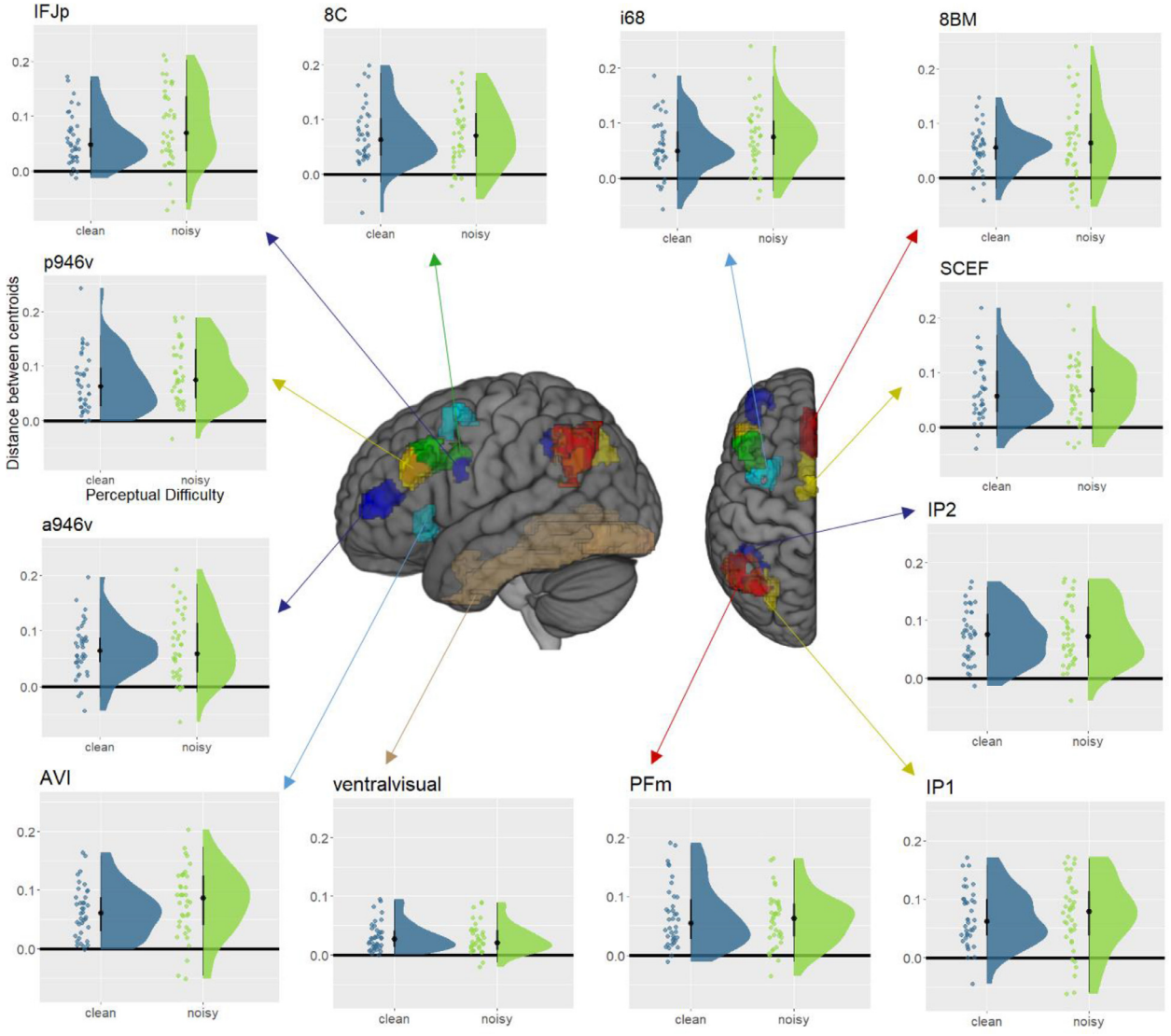

Fig. 5. *Category-level stimulus coding.* For each ROI, the distance between both category centroids in plotted, separately for clean and noisy trials. Each plot shows the median (black dot), estimated distribution (violin plot), and the raw data (dots), slighltly scattered for presentation purposes. Values above the black line indicate the presence of category signals.

reduction in category-level stimulus coding on noisy trials (BF10 = 0.1). Therefore, ventral visual cortex retained the same degree of category separation even under challenging perceptual conditions.

3.3. Hypothesis 2: stronger category signals on noisy trials in MD regions

We first tested whether MD regions encoded stimulus categories. As expected, we found strong evidence for category-level stimulus coding in all MD regions, both on clean and noisy trials (all BF10s > 150, Fig. 5). In a next step, we assessed whether category coding increased on noisy trials. Counter to our expectations, we found no increase in category coding in any MD region, all BF10s < 1.34. For some ROIs (SCEF, 8C, IP2, IP1, PFm), we even found evidence against any differences in category signals between clean and noisy trials, all BF10s < 0.24 (Fig. 5). Overall, we found no evidence for an adaptive strengthening of task-relevant category information under perceptually difficult conditions.

We then performed a post-hoc control analysis, in which we better controlled for potential behavioral effects of choice difficulty on these results. We first split the dataset into two sub-sets, one containing only trials from choice difficulty levels 1 and 2, the other only containing trials from choice difficulty levels 3 and 4. The main analysis was then repeated separately for each subset, and computed distances were then averaged. This analysis keeps choice difficulty effects smaller, and still allows us to compute category-level and stimulus-level distance measures. Results largely confirmed our original findings. We found strong evidence for category-level stimulus coding in all MD regions, both on clean and noisy trials (all BF10s > 150). Furthermore, we found no evidence for an increase in category coding in any ROI, all BF10s < 1.38. Evidence for an effect was marginally stronger in IFJp, BF10 = 2.94, but still too weak to interpret in the context of a post-hoc analysis.

We also repeated the main analysis in a different set MD ROIs, extracted from Fedorenko et al. (2013). Again, we found category-level stimulus coding in all MD regions on both clean an noisy trials (all BF10s > 150), and no evidence for an increase in category coding in any MD region (all BF10s < 1.07), confirming our original results.

3.4. Hypothesis 3: more clustering on noisy trials in MD regions

We also hypothesized that MD regions would de-emphasize task-irrelevant exemplar-level stimulus information in response to increased difficulty. We found stimulus representations to be more strongly clustered on noisy trials in PFC (IFJp, a946v), parietal cortex (IP1, IP2), and

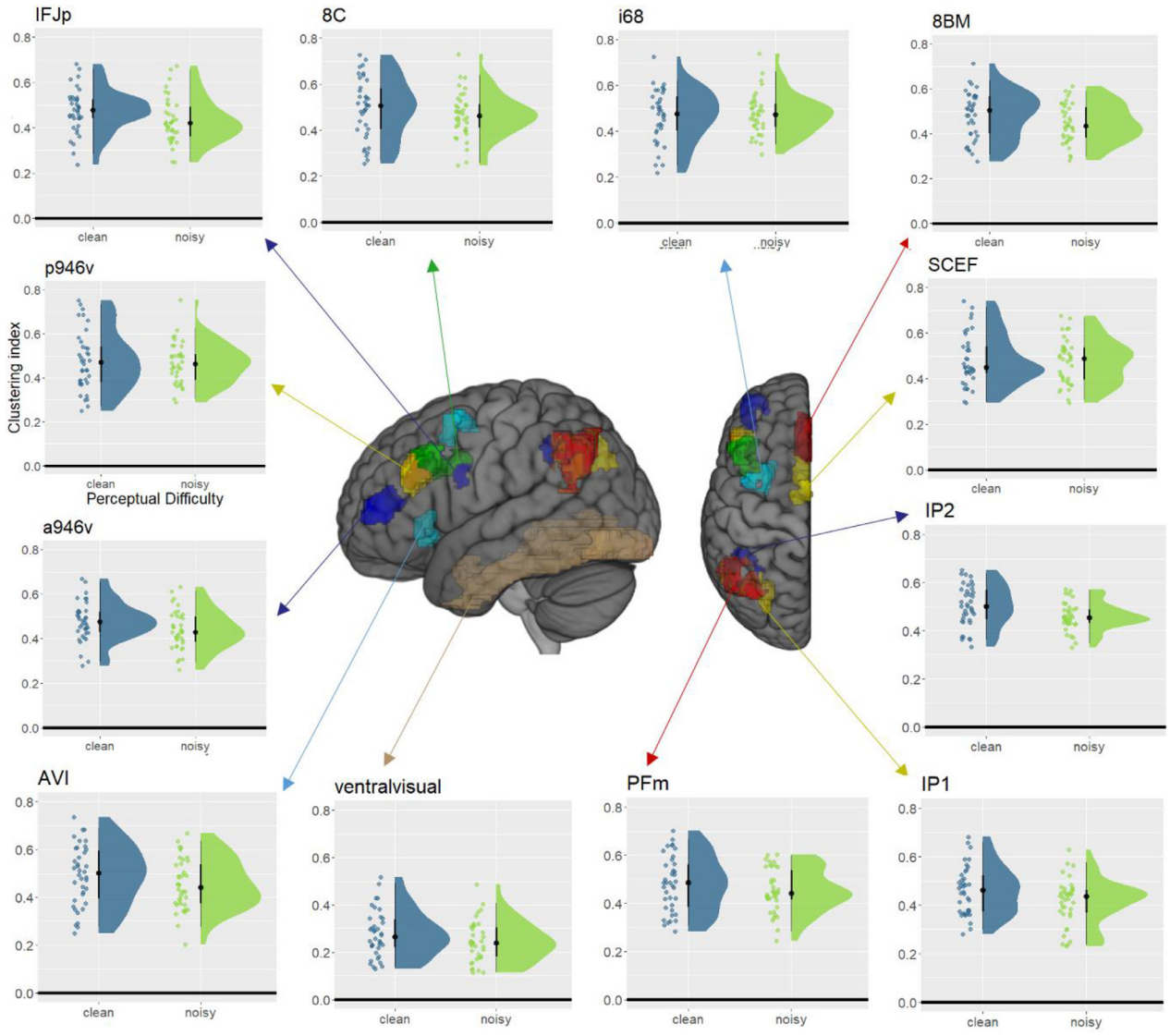

Fig. 6. *Exemplar-level stimulus clustering.* For each ROI, the average distance of each exemplar to their respective category centroid is plotted, separately for clean and noisy trials. Each plot shows the median (black dot), estimated distribution (violin plot), and the raw data (dots), slightly scattered for presentation purposes.

surprisingly ventral visual cortex (all BF10s > 3.42, Fig. 6). Evidence against any differences was found in PFC (i68 and p946v, all BF10s < 0.26).

Again, we performed a post-hoc control analysis, in which we analyzed choice difficulty levels 1 and 2 separately from levels 3 and 4 (see above). We found no evidence for stronger clustering in any ROI, including MD and ventral visual cortex (all BF10s < 1.41). This finding might seem somewhat surprising, but we believe it to mainly reflect a lack of statistical power. By splitting the whole data set into two subsets, the number of available data points was reduced by half, which significantly reduced statistical power. Somewhat weaker results would therefore be expected even if the true effect remained the same. Although we cannot fully exclude a potential effect of choice difficulty on these results, we believe that ultimately the lack of statistical power makes a clear interpretation difficult.

As before, we also repeated the main analysis using MD ROIs extracted from Fedorenko et al. (2013), confirming results in parietal cortex (IPS, BF10 = 95.18), but not in PFC (all BF10s < 0.31).

Overall, these results demonstrate that although category separation remained unaffected by the perceptual difficulty manipulation, exemplar-level stimulus information changed adaptively according to current perceptual difficulty conditions. Prefrontal, parietal, and visual brain regions showed more strongly clustered exemplar representations under perceptually difficult conditions, with parietal results being the most robust. While this has been expected in MD regions, finding this effect in ventral visual cortex has been surprising.

4. Discussion

In summary, we found evidence for adaptive stimulus coding in a visual classification task in parietal cortex (IP1, IP2), dlPFC (IFJp, a946v), and surprisingly ventral visual cortex. Initially, we hypothesized that MD regions would show stronger task-relevant category signals under perceptually difficult conditions, as a means to compensate for increased difficulty. Yet, we found no evidence for such an effect. We did find evidence for a change in task-irrelevant exemplar-level stimulus coding however. Increasing perceptual difficulty altered representational formats towards more clustered representations in parietal, prefrontal and visual brain regions.

Past research on perceptual decision-making and visual classification demonstrated that both visual and prefrontal brain regions encode stimulus information (Freedman et al., 2003; Jackson et al., 2017; Jackson and Woolgar, 2018), and we replicate these results here. While ventral visual cortex represents the full stimulus space, i.e.

information about both categories and individual exemplars (Eger et al., 2008; Kriegeskorte et al., 2008), higher-level brain regions such as the prefrontal cortex have been reported to carry little information about individual exemplars in both humans (Mok and Love, 2021) and non-human primates (Freedman et al., 2003; Freedman and Assad, 2006). These findings demonstrate a tuning of "perceptual" representations towards the task goal, successful categorization. Such abstract, "behavioral" representations emphasize task-relevant information (categories) and remove task-irrelevant information (exemplars). The design of our experiment allowed us to assess those two aspects of stimulus coding under changing perceptual difficulty conditions. First, we were able to determine the representational distance between the two categories used here (task-relevant category information). Second, we were able to determine to which degree individual exemplars within the same category were spread around the centroid of each category (task-irrelevant exemplar information). A larger spread indicates more dissimilar exemplar-level stimulus representations, a smaller spread indicates more similar and clustered representations.

In MD cortex, we expected to see increased category coding and more similar/clustered exemplar-level representations. In addition to previous findings, this hypothesis was informed by recent theories on adaptive coding (Badre et al., 2021; Fusi et al., 2016). The transformation of perceptual into behavioral stimulus representations makes coding more categorical (Brincat et al., 2018), and this essentially reflects a dimensionality reduction in neural representations. High-dimensional perceptual representations that carry information about the whole stimulus space are transformed into low-dimensional, behavioral representations that merely carry information about the task-relevant stimulus dimension. Recent theories suggest that high-dimensional representations are more easily separable, but also more susceptible to noise (Badre et al., 2021; Fusi et al., 2016). Low-dimensional representations are more robust to noise, suggesting they would be especially useful on noisy, perceptually difficult trials, where stimulus information is degraded.

We found evidence for category signals in MD and visual brain regions, but no evidence for an increase on noisy, as compared to clean, trials. In parietal cortex (IP1, IP2) we even found evidence against any differences, indicating that category coding was equally strong across perceptual difficulty levels. We can only speculate as to why we did not observe the expected effects here. One potential explanation might be that the overall effect size of category signals was low. Comparing Figs. 5 and 6 demonstrates that the distance between the category centroids was much smaller than the spread of individual exemplars around that centroid. Therefore, we cannot fully rule out that despite the large sample size, a modulation of such small effects remained too hard to detect. Recently it has been suggested that different types of difficulty manipulations engage the MD regions differently (Wen et al., 2018). Specifically, difficulty manipulations that limit or degrade incoming stimulus information (e.g. increased noise) might not recruit MD regions as much as manipulations that make stimulus processing harder (e.g. mental rotation, Han and Marois 2013). This would make sense if MD regions recruit additional attentional resources to compensate for increased processing demands (Duncan et al., 2020), but are not involved in refining stimulus representations themselves. From this perspective, degrading stimulus information might not have led to the strongest adaptive effects in MD regions, and it might be that using a more "cognitive" difficulty manipulation would lead to the expected enhancement of category signals. Clearly, this remains speculative at this point, and future research will be necessary to address these issues.

More interestingly, we did find evidence for adaptive changes to task-irrelevant exemplar-level stimulus coding in some MD regions (IP1, IP2, IFJp, a946v). Exemplars were clustered together more strongly under perceptually difficult conditions in these parietal and prefrontal regions. A post-hoc control analysis revealed that these effects might at least partially reflect choice difficulty effects, but the analysis was not statistically powerful enough to draw strong conclusions. Future research with optimized designs and even higher sample sizes will be necessary to resolve this issue. One might further argue that the stronger clustering was simply due to the perceptual difficulty manipulation, noisy stimuli were likely perceived as more similar to each other due to the visual degradation. If this were the case, we would expect to see an unspecific collapse of all representational distances, including the distance between category centroids though. Especially in parietal cortex (IP1, IP2), this was not the case. While we found evidence for stronger clustering of exemplars within a category, we found evidence against any differences in the distance between category centroids. Such a specific effect cannot be easily explained with a global signal reduction. Rather, it seems more likely that this is an adaptive response by MD regions to the increased perceptual difficulty of the task. Interestingly, the ventral visual cortex exhibited largely the same adaptive response to perceptual difficulty as the parietal cortex. There are some previous findings showing that visual brain regions carry information about e.g. behavior in perceptual decision-making tasks (Hebart et al., 2012), questioning its role as a purely "perceptual" brain region. Our findings add to this evidence by showing that ventral visual cortex exhibits adaptive responses that are highly similar to those of higher-level frontoparietal brain regions. It will be interesting to see whether a similar effect would be observed in a modified task in which difficulty is not manipulated by degrading stimuli visually, but rather by making their cognitive processing more demanding. If increased clustering is a general adaptive mechanism, we would expect to observe it in MD regions under different types of difficulty manipulations, but effects in visual regions might be specific to perceptual difficulty manipulations.

Overall, although our findings did not demonstrate an adaptive response in task-relevant category information in MD regions, they did demonstrate an adaptive response in task-irrelevant exemplar-level stimulus information. Interestingly, ventral visual cortex showed a response that was highly similar to some parietal and prefrontal brain regions. These results reveal how specific representational formats do and do not change under varying task demands, and thus provide evidence of *how* neural coding adapts to changing demands.

Declaration of Competing Interest

The authors declare no competing interests.

Credit authorship contribution statement

David Wisniewski: Conceptualization, Methodology, Software, Formal analysis, Investigation, Resources, Data curation, Writing – original draft, Writing – review & editing, Visualization, Project administration, Funding acquisition. **Carlos González-García:** Conceptualization, Methodology, Resources, Investigation, Writing – review & editing. **Silvia Formica:** Conceptualization, Resources, Investigation, Writing – review & editing. **Alexandra Woolgar:** Conceptualization, Methodology, Investigation, Writing – review & editing. **Marcel Brass:** Conceptualization, Methodology, Investigation, Writing – review & editing, Funding acquisition.

Data availability

Data and code is available online on the Open Science Framework: https://osf.io/pw8v6.

Acknowledgments

We would like to thank David Freedman for kindly sharing the stimulus material used in this study. DW was supported by the European Union's Horizon 2020 research and innovation program under the Marie Skłodowska-Curie grant agreement no. 665501, the Flemish Science Foundation (FWO, FWO.KAN.2019.0023.01), and the Special Research Fund of Ghent University. CGG was supported by the Spanish Ministry of Science and Innovation (IJC2019–040208-I). SF was supported by

the Einstein Foundation Berlin. AW was supported by Medical Research Council (U.K) intramural funding SUAG/052/G101400. MB was supported by an Einstein Strategic Professorship of the Einstein Foundation Berlin, and a GOA of the Special Research Fund of Ghent University (BOF.GOA.2017.0002.03).

References

Arbuckle, S.A., Yokoi, A., Pruszynski, J.A., Diedrichsen, J., 2019. Stability of representational geometry across a wide range of fMRI activity levels. Neuroimage 186, 155–163. doi:10.1016/j.neuroimage.2018.11.002.

Ashby, S.R., Zeithamova, D., 2022. Category-biased neural representations form spontaneously during learning that emphasizes memory for specific instances. J. Neurosci. 42 (5), 865–876. doi:10.1523/JNEUROSCI.1396-21.2021.

Assem, M., Glasser, M.F., Van Essen, D.C., Duncan, J., 2020. A domain-general cognitive core defined in multimodally parcellated human cortex. Cerebral Cortex 30 (8), 4361–4380. doi:10.1093/cercor/bhaa023.

Badre, D., Bhandari, A., Keglovits, H., Kikumoto, A., 2021. The dimensionality of neural representations for control. Curr. Opin. Behav. Sci. 38, 20–28. doi:10.1016/j.cobeha.2020.07.002.

Bode, S., Haynes, J.D., 2009. Decoding sequential stages of task preparation in the human brain. Neuroimage 45 (2), 606–613. doi:10.1016/j.neuroimage.2008.11.031.

Botvinick, M.M., Cohen, J.D., 2014. The computational and neural basis of cognitive control: charted territory and new frontiers. Cogn. Sci. 38 (6), 1249–1285. doi:10.1111/cogs.12126.

Brincat, S.L., Siegel, M., von Nicolai, C., Miller, E.K., 2018. Gradual progression from sensory to task-related processing in cerebral cortex. Proc. Natl. Acad. Sci. 115 (30), E7202–E7211. doi:10.1073/pnas.1717075115.

Desimone, R., Duncan, J., 1995. Neural mechanisms of selective visual attention. Annu. Rev. Neurosci. 18 (1), 193–222. doi:10.1146/annurev.ne.18.030195.001205.

Duncan, J., 2010. The multiple-demand (MD) system of the primate brain: mental programs for intelligent behaviour. Trends Cogn. Sci. (Regul. Ed.) 14 (4), 172–179. doi:10.1016/j.tics.2010.01.004.

Duncan, J., 2013. The structure of cognition: attentional episodes in mind and brain. Neuron 80 (1), 35–50. doi:10.1016/j.neuron.2013.09.015.

Duncan, J., Assem, M., Shashidhara, S., 2020. Integrated intelligence from distributed brain activity. Trends Cogn. Sci. (Regul. Ed.) doi:10.1016/j.tics.2020.06.012.

Eger, E., Ashburner, J., Haynes, J.D., Dolan, R.J., Rees, G., 2008. FMRI activity patterns in human LOC carry information about object exemplars within category. J. Cogn. Neurosci. 20 (2), 356–370. doi:10.1162/jocn.2008.20019.

Etzel, J.A., Cole, M.W., Zacks, J.M., Kay, K.N., Braver, T.S., 2016. Reward motivation enhances task coding in frontoparietal cortex. Cerebral Cortex 26 (4), 1647–1659. doi:10.1093/cercor/bhu327.

Fedorenko, E., Duncan, J., Kanwisher, N., 2013. Broad domain generality in focal regions of frontal and parietal cortex. Proc. Natl. Acad. Sci. 110 (41), 16616–16621. doi:10.1073/pnas.1315235110.

Freedman, D.J., Assad, J.A., 2006. Experience-dependent representation of visual categories in parietal cortex. Nature 443 (7107), 85–88. doi:10.1038/nature05078.

Freedman, D.J., Riesenhuber, M., Poggio, T., Miller, E.K., 2003. A comparison of primate prefrontal and inferior temporal cortices during visual categorization. J. Neurosci. 23 (12), 5235–5246. doi:10.1523/JNEUROSCI.23-12-05235.2003.

Friston, K.J., Holmes, A.P., Worsley, K.J., Poline, J.-P., Frith, C.D., Frackowiak, R.S., 1994. Statistical parametric maps in functional imaging: a general linear approach. Hum.Brain Mapp. 2 (4), 189–210.

Fusi, S., Miller, E.K., Rigotti, M., 2016. Why neurons mix: high dimensionality for higher cognition. Curr. Opin. Neurobiol. 37, 66–74. doi:10.1016/j.conb.2016.01.010.

Fuster, J.M., 2000. Executive frontal functions. Exp. Brain Res. 133 (1), 66–70. doi:10.1007/s002210000401.

Glasser, M.F., Coalson, T.S., Robinson, E.C., Hacker, C.D., Harwell, J., Yacoub, E., Ugurbil, K., Andersson, J., Beckmann, C.F., Jenkinson, M., Smith, S.M., Van Essen, D.C., 2016. A multi-modal parcellation of human cerebral cortex. Nature 536 (7615), 171–178. doi:10.1038/nature18933.

Han, S.W., Marois, R., 2013. Dissociation between process-based and data-based limitations for conscious perception in the human brain. Neuroimage 64, 399–406. doi:10.1016/j.neuroimage.2012.09.016.

Haynes, J.D., 2015. A primer on pattern-based approaches to fMRI: principles, pitfalls, and perspectives. Neuron 87 (2), 257–270. doi:10.1016/j.neuron.2015.05.025.

Hebart, M.N., Donner, T.H., Haynes, J.D., 2012. Human visual and parietal cortex encode visual choices independent of motor plans. Neuroimage 63 (3). doi:10.1016/j.neuroimage.2012.08.027, Article 3.

Hebart, M.N., Görgen, K., Haynes, J.-.D., 2014. The Decoding Toolbox (TDT): a versatile software package for multivariate analyses of functional imaging data. Front. Neuroinform. 8, 88. doi:10.3389/fninf.2014.00088.

Heekeren, H.R., Marrett, S., Bandettini, P.A., Ungerleider, L.G., 2004. A general mechanism for perceptual decision-making in the human brain. Nature 431 (7010). doi:10.1038/nature02966, Article 7010.

Jackson, J., Feredoes, E., Rich, A.N., Lindner, M., Woolgar, A., 2021. Concurrent neuroimaging and neurostimulation reveals a causal role for dlPFC in coding of task-relevant information. Commun. Biol. 4 (1). doi:10.1038/s42003-021-02109-x, Article 1.

Jackson, J., Rich, A.N., Williams, M.A., Woolgar, A., 2017. Feature-selective attention in frontoparietal cortex: multivoxel codes adjust to prioritize task-relevant information. J. Cogn. Neurosci. 29 (2), 310–321. doi:10.1162/jocn_a_01039.

Jackson, J., Woolgar, A., 2018. Adaptive coding in the human brain: distinct object features are encoded by overlapping voxels in frontoparietal cortex. Cortex 108, 25–34. doi:10.1016/j.cortex.2018.07.006.

Kamitani, Y., Tong, F., 2006. Decoding seen and attended motion directions from activity in the human visual cortex. Curr. Biol. 16 (11), 1096–1102. doi:10.1016/j.cub.2006.04.003.

Kriegeskorte, N., Kievit, R.A., 2013. Representational geometry: integrating cognition, computation, and the brain. Trends Cogn. Sci. (Regul. Ed.) 17 (8). doi:10.1016/j.tics.2013.06.007, Article 8.

Kriegeskorte, N., Mur, M., Bandettini, P., 2008a. Representational similarity analysis – connecting the branches of systems neuroscience. Front. Syst. Neurosci. 2. doi:10.3389/neuro.06.004.2008.

Kriegeskorte, N., Mur, M., Ruff, D.A., Kiani, R., Bodurka, J., Esteky, H., Tanaka, K., Bandettini, P.A., 2008b. Matching categorical object representations in inferior temporal cortex of man and monkey. Neuron 60 (6), 1126–1141. doi:10.1016/j.neuron.2008.10.043.

Li, S., Ostwald, D., Giese, M., Kourtzi, Z., 2007. Flexible coding for categorical decisions in the human brain. J. Neurosci. 27 (45), 12321–12330. doi:10.1523/JNEUROSCI.3795-07.2007.

Linares, D., López-Moliner, J., 2016. Quickpsy: An R package to fit psychometric functions for multiple groups. R J. 8 (1), 122–131.

Loose, L.S., Wisniewski, D., Rusconi, M., Goschke, T., Haynes, J.D., 2017. Switch-independent task representations in frontal and parietal cortex. J. Neurosci. 37 (33), 8033–8042. doi:10.1523/JNEUROSCI.3656-16.2017.

McKee, J.L., Riesenhuber, M., Miller, E.K., Freedman, D.J., 2014. Task dependence of visual and category representations in prefrontal and inferior temporal cortices. J. Neurosci. 34 (48), 16065–16075. doi:10.1523/JNEUROSCI.1660-14.2014.

Miller, E.K., 2000. The prefontral cortex and cognitive control. Nat. Rev. Neurosci. 1 (1), 59–65.

Mok, R.M., Love, B.C., 2021. Abstract neural representations of category membership beyond information coding stimulus or response. J. Cogn. Neurosci. 1–17. doi:10.1162/jocn_a_01651.

Momennejad, I., Haynes, J.D., 2012. Human anterior prefrontal cortex encodes the 'what' and 'when' of future intentions. Neuroimage 61 (1), 139–148. doi:10.1016/j.neuroimage.2012.02.079.

Momennejad, I., Haynes, J.D., 2013. Encoding of prospective tasks in the human prefrontal cortex under varying task loads. J. Neurosci. 33 (44), 17342–17349. doi:10.1523/JNEUROSCI.0492-13.2013.

Nili, H., Wingfield, C., Walther, A., Su, L., Marslen-Wilson, W., Kriegeskorte, N., 2014. A toolbox for representational similarity analysis. PLoS Comput. Biol. 10 (4), e1003553. doi:10.1371/journal.pcbi.1003553.

Peirce, J.W., 2007. PsychoPy—psychophysics software in Python. J. Neurosci. Methods 162 (1), 8–13. doi:10.1016/j.jneumeth.2006.11.017.

Wagenmakers, E.J., 2007. A practical solution to the pervasive problems of p values. Psychon. Bull. Rev. 14 (5), 779–804. doi:10.3758/BF03194105.

Walther, A., Nili, H., Ejaz, N., Alink, A., Kriegeskorte, N., Diedrichsen, J., 2016. Reliability of dissimilarity measures for multi-voxel pattern analysis. Neuroimage 137, 188–200. doi:10.1016/j.neuroimage.2015.12.012.

Wen, T., Mitchell, D.J., Duncan, J., 2018. Response of the multiple-demand network during simple stimulus discriminations. Neuroimage 177, 79–87. doi:10.1016/j.neuroimage.2018.05.019.

Wisniewski, D., 2018. Context-dependence and context-invariance in the neural coding of intentional action. Front. Psychol. 9. doi:10.3389/fpsyg.2018.02310.

Wisniewski, D., Forstmann, B., Brass, M., 2019. Outcome contingency selectively affects the neural coding of outcomes but not of tasks. Sci. Rep. 9 (1), 1–15. doi:10.1038/s41598-019-55887-0.

Wisniewski, D., Goschke, T., Haynes, J.D., 2016. Similar coding of freely chosen and externally cued intentions in a fronto-parietal network. Neuroimage 134, 450–458. doi:10.1016/j.neuroimage.2016.04.044.

Wisniewski, D., Reverberi, C., Momennejad, I., Kahnt, T., Haynes, J.-.D., 2015. The role of the parietal cortex in the representation of task–reward associations. J. Neurosci. 35 (36), 12355–12365. doi:10.1523/JNEUROSCI.4882-14.2015.

Woolgar, A., Afshar, S., Williams, M.A., Rich, A.N., 2015a. Flexible coding of task rules in frontoparietal cortex: an adaptive system for flexible cognitive control. J. Cogn. Neurosci. 1–17. doi:10.1162/jocn_a_00827.

Woolgar, A., Hampshire, A., Thompson, R., Duncan, J., 2011a. Adaptive coding of task-relevant information in human frontoparietal cortex. J. Neurosci. 31 (41), 14592–14599. doi:10.1523/JNEUROSCI.2616-11.2011.

Woolgar, A., Jackson, J., Duncan, J., 2016. Coding of visual, auditory, rule, and response information in the brain: 10 years of multivoxel pattern analysis. J. Cogn. Neurosci. 28 (10), 1433–1454. doi:10.1162/jocn_a_00981.

Woolgar, A., Thompson, R., Bor, D., Duncan, J., 2011b. Multi-voxel coding of stimuli, rules, and responses in human frontoparietal cortex. Neuroimage 56 (2), 744–752. doi:10.1016/j.neuroimage.2010.04.035.

Woolgar, A., Williams, M.A., Rich, A.N., 2015b. Attention enhances multi-voxel representation of novel objects in frontal, parietal and visual cortices. Neuroimage 109, 429–437. doi:10.1016/j.neuroimage.2014.12.083.

Zhang, J., Kriegeskorte, N., Carlin, J.D., Rowe, J.B., 2013. Choosing the rules: distinct and overlapping frontoparietal representations of task rules for perceptual decisions. J. Neurosci. 33 (29), 11852–11862. doi:10.1523/JNEUROSCI.5193-12.2013.